Journal of Physiology (1993), **463**, *pp.* 391–407
With 6 figures
Printed in Great Britain

CHARACTERIZATION OF SYNAPTICALLY ELICITED $GABA_B$ RESPONSES USING PATCH-CLAMP RECORDINGS IN RAT HIPPOCAMPAL SLICES

BY THOMAS S. OTIS, YVES DE KONINCK AND ISTVAN MODY*

From the Department of Neurology and Neurological Sciences, Stanford University Medical Center, Room MO 16, Stanford, CA 94305, USA

(*Received 9 April 1992*)

SUMMARY

1. Tight-seal, whole-cell voltage clamp recording techniques were used to characterize monosynaptically evoked $GABA_B$ currents in adult rat brain slices maintained at 34–35 °C. Responses were recorded from granule cells of the dentate gyrus following the blockade of 6-cyano-7-nitroquinoxaline-2,3-dione (CNQX)-, D-2-amino-5-phosphonovaleric acid (D-AP5)- and picrotoxin-sensitive fast synaptic transmission, so that the remaining synaptic currents could be studied in isolation.

2. Under these conditions, stimulation in the molecular layer elicited a slow outward current which was blocked by the selective $GABA_B$ antagonist CGP 35348 in a concentration-dependent manner (200–800 μM). This current was absent in recordings made with pipettes containing 10–15 mM of the lidocaine derivative QX-314 or when caesium was substituted for K^+.

3. Increasing the $[K^+]_o$ e-fold (from 2·5 to 6·8 mM) shifted the reversal potential of the $GABA_B$ current from $-97{\cdot}9$ to $-73{\cdot}2$ mV, as predicted by the Nernst equation. Peak conductance was constant, but in 6·8 mM $[K^+]_o$ at voltages hyperpolarized to E_K (equilibrium potential for potassium), a small outward rectification was evident.

4. The time course of the current could be described by fourth-power exponential activation kinetics with double exponential inactivation. At 34–35 °C, the average activation time constant (τ_m) was 45·2 ms, while the two inactivation time constants (τ_{h_1} and τ_{h_2}) were 110·2 and 516·2 ms, with corresponding weighting factors (w_{h_1} and w_{h_2}) of 0·84 and 0·16, respectively. The Q_{10} (temperature coefficient) values for these time constants were between 1·82 and 2·31. Neither τ_m, nor τ_{h_1} and τ_{h_2} were voltage dependent in the range from -45 to -95 mV.

5. Paired-pulse depression of the $GABA_B$ current was studied by giving identical conditioning and test stimuli over a wide range (50–5000 ms) of interstimulus intervals (ISIs). The maximal depression (48%) occurred at 200 ms ISI, and the depression lasted for over 5 s. The magnitude of paired-pulse depression was not dependent on the postsynaptic membrane potential.

6. Application of the competitive antagonist CGP 35348 such that the peak current was diminished by approximately 50% had no effect on the activation or inactivation kinetics of the current. Similarly, during paired-pulse depression the

* To whom correspondence should be sent.

MS 1276

kinetics of test currents were identical to those of conditioning currents. These findings support the hypothesis that the mechanism responsible for paired-pulse depression involves a reduction in neurotransmitter release without postsynaptic alterations in K^+ channel activation/inactivation kinetics.

7. Comparison of the time course of the postsynaptic $GABA_B$ current with that of the paired-pulse depression indicates that a presynaptic conductance identical to the postsynaptic $GABA_B$ K^+ conductance is not sufficient alone to depress neurotransmitter release by hyperpolarizing the presynaptic terminal.

INTRODUCTION

Two types of GABA receptors, termed $GABA_A$ and $GABA_B$ receptors, are thought to exist in the mammalian central nervous system (CNS) (for review see Bowery, 1989; Nicoll, Malenka & Kauer, 1990). Both types of receptors are often found on excitatory (Newberry & Nicoll, 1985) and inhibitory neurones (Lacaille, 1991). While $GABA_A$ receptors mediate fast inhibitory synaptic transmission and the $IPSP/C_A$ (Nicoll *et al.* 1990), $GABA_B$ receptors give rise to a much slower synaptic response, and in some cases, are thought to produce inhibition through the indirect activation of a K^+ conductance ($IPSP/C_B$, Newberry & Nicoll, 1985; Gähwiler & Brown, 1985; Misgeld, Müller & Brunner, 1989; Nicoll *et al.* 1990). The postsynaptic potential resulting from this $GABA_B$ receptor-activated K^+ conductance (Dutar & Nicoll, 1988*a*), often termed the late IPSP or $IPSP_B$, has been shown to be blocked by pretreatment with pertussis toxin (Dutar & Nicoll, 1988*b*), and activated by intracellular application of GTPγS (Thalmann, 1988). Thus, the $GABA_B$ receptor is likely to be a member of the seven-transmembrane domain receptor family, which includes receptors coupled via GTP-binding proteins to various intracellular enzymes and ion channels (Gilman, 1987).

In contrast to the wealth of information regarding the function of the $GABA_A$ receptor–channel complex, very little is known about the K^+ conductance activated by $GABA_B$ receptors (Nicoll *et al.* 1990). The precise steps in the transduction pathway from G-protein activation to the K^+ channel opening are poorly understood, though the time course of the synaptic response suggests a direct interaction between ion channel and G-protein (Thalmann, 1988), as has been hypothesized for the activation of some cardiac (Yatani *et al.* 1988) and brain (VanDongen *et al.* 1988; Miyake, Christie & North, 1989) K^+ channels. Previous studies have described $GABA_B$ agonist-activated currents (Gähwiler & Brown, 1985), GABA-activated K^+ channels (Premkumar, Chung & Gage, 1990; Gage, 1992), or G-protein-activated single K^+ channel currents (VanDongen *et al.* 1988; Miyake *et al.* 1989), but a characterization of the kinetics and voltage dependence of the synaptically activated $GABA_B$ current is lacking. In fact, there are presently no kinetic analyses of synaptically elicited G-protein-activated currents.

Of the three studies concerning G-protein-activated single K^+ channels in central neurones (VanDongen *et al.* 1988; Miyake *et al.* 1989; Premkumar *et al.* 1990), only one (Premkumar *et al.* 1990) has specifically characterized $GABA_B$ receptor-activated K^+ channels. Furthermore, it is not clear whether the GABA- or baclofen-activated single K^+ channels described in these studies underlie the $IPSP_B$ recorded

in brain slices. A primary aim of our study was to characterize the kinetics and voltage dependence of the synaptically activated $GABA_B$ current.

Another aim was to examine the paired-pulse depression of the $GABA_B$ current. Like the IPSP/C_A (Davies, Davies & Collingridge, 1990; Harrison, 1990; Otis & Mody, 1992*a*), the IPSP/C_B shows a similar frequency-dependent depression (Davies *et al.* 1990). Though the precise mechanism of this paired-pulse depression remains unclear, it appears to involve activation of $GABA_B$ receptors located on presynaptic neurones (Bowery *et al.* 1980; Dutar & Nicoll, 1988*b*; Harrison, Lange & Barker, 1988; Deisz & Prince, 1989; Misgeld *et al.* 1989; Davies *et al.* 1990). Evidence supporting this model of $GABA_B$ receptor-mediated presynaptic inhibition for both the EPSP (Dutar & Nicoll, 1988*b*; Thompson & Gähwiler, 1992) and the IPSP/C_A (Davies *et al.* 1990; Harrison, 1990; Otis & Mody, 1992*a*; Thompson & Gähwiler, 1992), has come from experiments using selective agonists or antagonists for $GABA_B$ receptors. Such experiments cannot be performed on the IPSP/C_B, thus it has been difficult to rule out postsynaptic contributions such as desensitization to the mechanism of paired-pulse depression of $GABA_B$ responses. Therefore, we examined the voltage dependence and the kinetics of the postsynaptic $GABA_B$ conductance during paired-pulse depression. By comparing the kinetics of the postsynaptic current with the time course of the paired-pulse depression, constraints could be placed on the possible mechanisms responsible for presynaptic inhibition of GABA release.

METHODS

Slice preparation

Recordings were made from granule cells of the dentate gyrus in coronal half-brain slices (400 μm thick) obtained from adult (postnatal day 60+; 200–400 g) Wistar rats. Briefly, following sodium pentobarbitone anaesthesia (60 mg kg^{-1}, I.P.), animals were decapitated, the brain quickly dissected and immersed for 1–2 min in cold (4 °C) artificial cerebrospinal fluid (ACSF) solution. Coronal whole-brain slices were prepared with a Vibratome (Lancer Series 1000). The storage of slices and type of recording chamber used were previously described in detail (Staley, Otis & Mody, 1992; Otis & Mody, 1992*b*).

The ACSF contained (mM): 126 NaCl, 2·5 KCl, 2 $CaCl_2$, 2 $MgCl_2$, 26 $NaHCO_3$, 1·25 NaH_2PO_4, 10 glucose, 0·03–0·04 D-AP5 (D-2-amino-5-phosphonovaleric acid), 0·01 CNQX (6-cyano-7-nitroquinoxaline-2,3-dione) and 0·075 picrotoxin (except for the experiments using 6·8 mM $[K^+]_o$, in which an additional 4·3 mM KCl was added to the ACSF, and those experiments measuring $GABA_A$ currents, in which picrotoxin was omitted) continuously bubbled with 95% O_2–5% CO_2 (pH 7·35±0·05). Drugs were added to the ACSF at the concentrations indicated. CGP 35348 was a generous gift of Ciba Geigy Pharmaceuticals Ltd, Basel, Switzerland. All other chemicals were purchased from Sigma except CNQX (Tocris Neuramin, Bristol, England), D-AP5 (Cambridge Research Biochemicals, Natick, MA, USA and Tocris Neuramin), 2-hydroxy-saclofen (Cambridge Research Biochemicals), and *N*(2,6-dimethylphenylcarbamoylmethyl)triethylammonium bromide (QX-314, generous gift of Astra Pharmaceuticals).

Whole-cell recordings

Whole-cell voltage clamp recordings were obtained using borosilicate glass capillaries with an inner filament (KG-33, 1·12 mm i.d., 1·5 mm o.d., Garner Glass) pulled to 1·5–3 μm outer tip diameters (0·5–1 μm diameter of the lumen) using a two stage vertical Narishige PP-83 puller. Intracellular solutions were either (mM) 135 potassium gluconate, 10 Hepes, 2 $MgCl_2$, 2 MgATP, and 0·2 Tris-GTP to measure $GABA_B$ currents; or 135 CsCl, 10 Hepes and 2 $MgCl_2$ for the $GABA_A$ currents. All solutions were titrated to pH 7·2 with KOH (or CsOH). Additional pipette contents will be noted in the text, and sometimes included 10 mM QX-314 or 11 mM BAPTA (1,2-bis(*O*-aminophenoxy)ethane-*N*,*N*,*N*′,*N*′-tetracetic acid) 1 mM $CaCl_2$. Total osmolality for all intracellular

solutions ranged from 255 to 285 mosmol kg^{-1} as measured on a Wescor 5500 vapour pressure osmometer.

The method for obtaining gigaseal recordings was described in detail elsewhere (Otis, Staley & Mody, 1991; Otis & Mody, 1992*b*; Staley *et al.* 1992). For those recordings made with potassium gluconate-based solutions, a junction potential of 11 mV was subtracted from the membrane potential values (Otis & Mody, 1992*a*). An activity coefficient of 0·75 for potassium gluconate (Vanysek, 1988) was used to determine the E_K (equilibrium potential for potassium) of −98 mV in 2·5 mM $[K^+]_o$ and −72 mV in 6·8 mM $[K^+]_o$.

Postsynaptic $GABA_B$ currents (and postsynaptic $GABA_A$ currents, cf. Fig. 6) were evoked using bipolar stimulating electrodes which were placed in the middle of the molecular layer of the dentate gyrus, 1–2 mm from the recording site. Constant current stimulus intensities ranging from 100 to 300 μA in amplitude and 20–200 μs in duration reliably evoked $GABA_B$ currents in granule cells. Most experiments were performed such that the peak evoked current was 70–100% of the maximum evoked current. No systematic differences in the kinetics of the current ($n = 5$), or in its sensitivity to antagonists ($n = 3$) were seen for different stimulus intensities.

Data analysis and curve fitting

All analog DC signals were digitized at 44 kHz (Neurocorder, NeuroData) and stored on a videotape for later analysis. Off-line, the recordings were low-pass filtered at DC to 0·3–1 kHz (−3 dB, 8-pole Bessel, Frequency Devices 9002), sampled (1–2 kHz), and analysed on an IBM-AT compatible microcomputer using the Strathclyde Electrophysiology software (courtesy of J. Dempster, University of Strathclyde, Glasgow), and software developed by Y.D.K. Statistical analyses included analysis of variance and the post-ANOVA (analysis of variance) Tukey's test.

The evoked postsynaptic $GABA_B$ currents were best fitted with a fourth-power exponential kinetic equation with a double inactivation process of the form:

$$I(t) = A[1-\exp(-t/\tau_m)]^4 [Aw_{h_1} \exp(-t/\tau_{h_1}) + Aw_{h_2} \exp(-t/\tau_{h_2})],$$

where $I(t)$ is current as a function of time, w_{h_1} and w_{h_2} (where $A = Aw_{h_1} + Aw_{h_2}$) are weighting factors, τ_m is the time constant of the activation parameter and τ_{h_1} and τ_{h_2} are the time constants of the inactivation parameters. This formulation is similar to a Hodgkin–Huxley type of formulation $[m^4(h_1+h_2)]$, and assumes an equilibrium activation (m_∞) value of 1 and an equilibrium inactivation value (h_∞) of zero. Unlike the original Hodgkin–Huxley description, however, there is no implied voltage dependence to any of the parameters. As a convention, we will use the Hodgkin–Huxley notation throughout this paper to refer to the time constants of activation and inactivation.

Curves were fitted by a least-squares method based on a Simplex algorithm (Caceci & Cacheris, 1984). For a given power of the activation parameter (m), each of the remaining parameters Aw_{h_1}, Aw_{h_2}, τ_m, τ_{h_1} and τ_{h_2} were allowed to vary freely within the Simplex routine. In some cases, rapidly decaying (5–15 ms) inward currents followed the stimulus artifacts (Figs 4*A* and *B* and 5*B–D*). These currents showed no voltage dependence (e.g. Fig. 5*B–D*) and, when necessary, were digitally subtracted before the curve fitting. Equivalent fits were obtained from traces with subtracted artifacts and traces without such artifacts (e.g. Fig. 2*B*).

RESULTS

The following results were obtained from recordings in over sixty dentate gyrus granule cells from adult rat brain slices. Cells recorded with the pipette solutions described in the methods were routinely maintained in excess of 1·5 h without any decrement in synaptic currents.

Pharmacological isolation and identification of the $GABA_B$ current

All recordings were made in extracellular solutions containing 10 μM CNQX, 30–40 μM D-AP5, and 75 μM picrotoxin (except Fig. 4*C*) which abolished fast synaptic currents, leaving only a slow outward current when voltage clamped near the resting membrane potential of the granule cells (cf. Staley & Mody, 1992).

This response was identified as a pure $GABA_B$ receptor-activated current by its sensitivity to the selective $GABA_B$ antagonist CGP 35348 (Olpe *et al.* 1990). More than 90% of the current was antagonized by bath application of CGP 35348 at concentrations above 200 μM (200–800 μM, $n = 5$). In related experiments, bath application of the $GABA_B$ receptor antagonist 2-hydroxy-saclofen (0·5–1 mM) also blocked the current ($n = 3$). Finally, the current could be blocked by intracellular agents such as 10–15 mM QX-314 ($n = 3$, Nathan, Jensen & Lambert, 1990; Otis & Mody, 1992*a*) or substitution of the K^+ in the pipette solutions by Cs^+ ($n = 12$, Gähwiler & Brown, 1985).

Voltage dependence of the $GABA_B$ current

Both a linear relationship between the peak synaptic $GABA_B$ response and membrane voltage (Thalmann, 1988; Davies *et al.* 1990), and a rectifying $GABA_B$ conductance (Gähwiler & Brown, 1985; Crunelli & Leresche, 1991) have been described. To assess the amount of rectification as well as the dependence of the current on $[K^+]_o$, we measured the peak amplitude of the isolated $GABA_B$ currents in granule cells over a range of voltages in $[K^+]_o$ of either 2·5 or 6·8 mM. For each cell, regression lines were fitted to the *I–V* plots so that the average slope conductances and reversal potentials could be calculated. Because of the variability in slope conductance between neurones, peak currents within a given neurone were normalized to the peak current recorded in that cell at either −75 mV (2·5 mM $[K^+]_o$) or −55 mV (6·8 mM $[K^+]_o$). These normalized measurements were then averaged across all cells to give the plots of peak $GABA_B$ current *versus* voltage shown in Fig. 1*A* and *B*.

In 2·5 mM $[K^+]_o$, the *I–V* relationship was linear in the voltage range −45 mV to −110 mV, and the regression line fitted to the data gave a correlation coefficient of 0·992, and showed a reversal potential of −94·2 mV. The mean slope conductance was 1·52 ± 0·16 nS (range 0·82–2·5 nS, $n = 9$). The average reversal potential obtained from individual regression analysis for each cell was −97·9 ± 1·7 mV ($n = 9$), identical to the calculated E_K of −98 mV. Traces recorded from a representative cell are displayed in Fig. 1*C*, along with an *I–V* plot shown in the inset.

Plots of inward currents measured in 6·8 mM $[K^+]_o$ uncovered an outward rectification in four out of seven neurones, as demonstrated in the average *I–V* relation seen in Fig. 1*B*. The remaining neurones (3 out of 7) showed linear *I–V* curves. The linear outward portion of the composite *I–V* plot showed a mean slope conductance of 2·69 ± 0·52 nS, (range 1·2–6·3 nS, $n = 7$), and the average reversal potential obtained from individual regression fits (linear portion of the *I–V* plot) to seven neurones was −73·2 ± 0·9 mV ($E_K = -72$ mV). Data from one of the three cells displaying a linear *I–V* relation is shown in Fig. 1*D*.

Kinetics of the $GABA_B$ current

Synaptic $GABA_B$ currents never rose from the baseline without a substantial delay (range 12–20 ms) following the stimulation artifact, and when well resolved, showed a sigmoidal rising phase. The decay of the current was best fitted by a double exponential. These characteristics could be accounted for by the product of a fourth-power exponential function for the activation, and the sum of two exponentials for

the inactivation or decay of the current (Fig. 2*A*). Neither the sum of rising and decaying exponential equations, nor an α-function could accurately describe the average current traces.

The best fits required a 10 ms 'lag' from the beginning of the stimulus artifact to the start of the curve. This 'lag' was included to account for a combination of spike

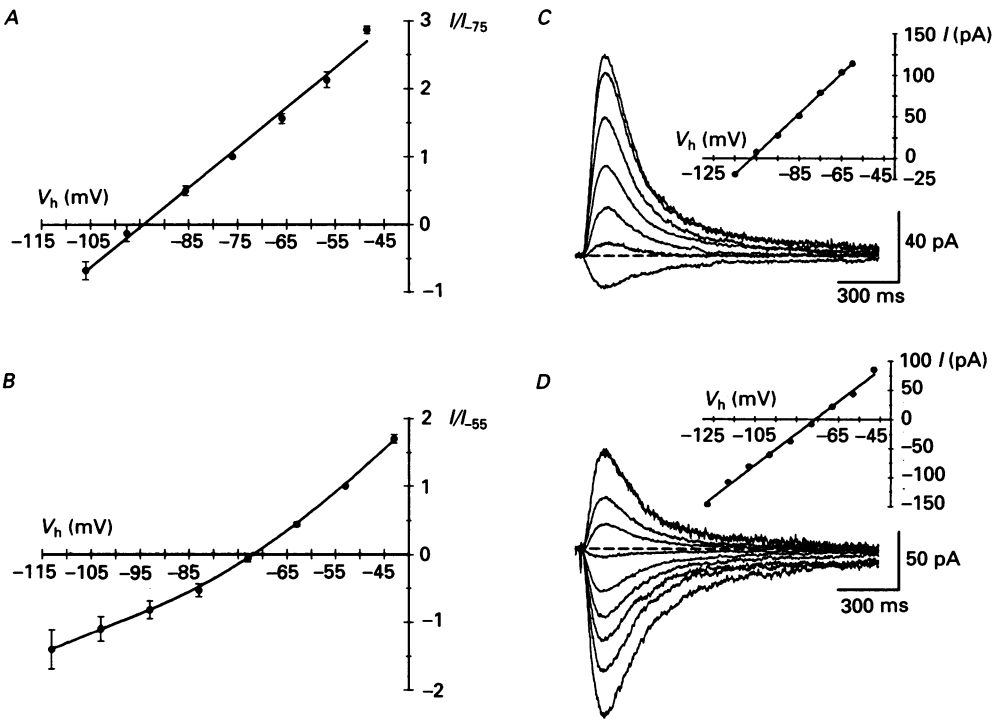

Fig. 1. The mean current *versus* voltage (V_h) relationship for the $GABA_B$ current shifts with changes in $[K^+]_o$, and at hyperpolarized potentials, rectifies in the outward direction. The *I–V* plots shown in *A* (2·5 mM $[K^+]_o$) and *B* (6·8 mM $[K^+]_o$) have been constructed by binning measurements in 10 mV bins, and within each cell, normalizing to the measurement at either −75 mV (2·5 mM) or −55 mV (6·8 mM). The *x*-axis values for each bin are the mean membrane potentials from all measurements within that bin. Standard error bars are displayed where they are larger than the symbols. Current traces recorded at a range of holding potentials for a cell recorded in 2·5 mM $[K^+]_o$ (*C*) and in 6·8 mM $[K^+]_o$ (*D*) are displayed with *I–V* plots as insets (see text). Each trace is the average of two or three responses.

conduction in the presynaptic neurone and the synaptic delay (2–4 ms after the stimulation artifact, as measured during extracellular field potential experiments) and a delay corresponding to the activation of postsynaptic G-proteins, estimated to be 6–8 ms based on kinetic measurements of receptor–G-protein interaction in other systems (cf. Vuong, Chabre & Stryer, 1984). Thus, a total 'lag' of approximately 10 ms after the beginning of the stimulus artifact was considered to be time zero for all of the fits performed at 34–35 °C. At room temperature, the 6–8 ms G-protein component of the 'lag' was doubled, such that the total 'lag' was 16 ms. If the lag time corresponds to the duration of all steps prior to activated G-proteins, then the activation time constants accurately reflect the activation of the K^+ currents.

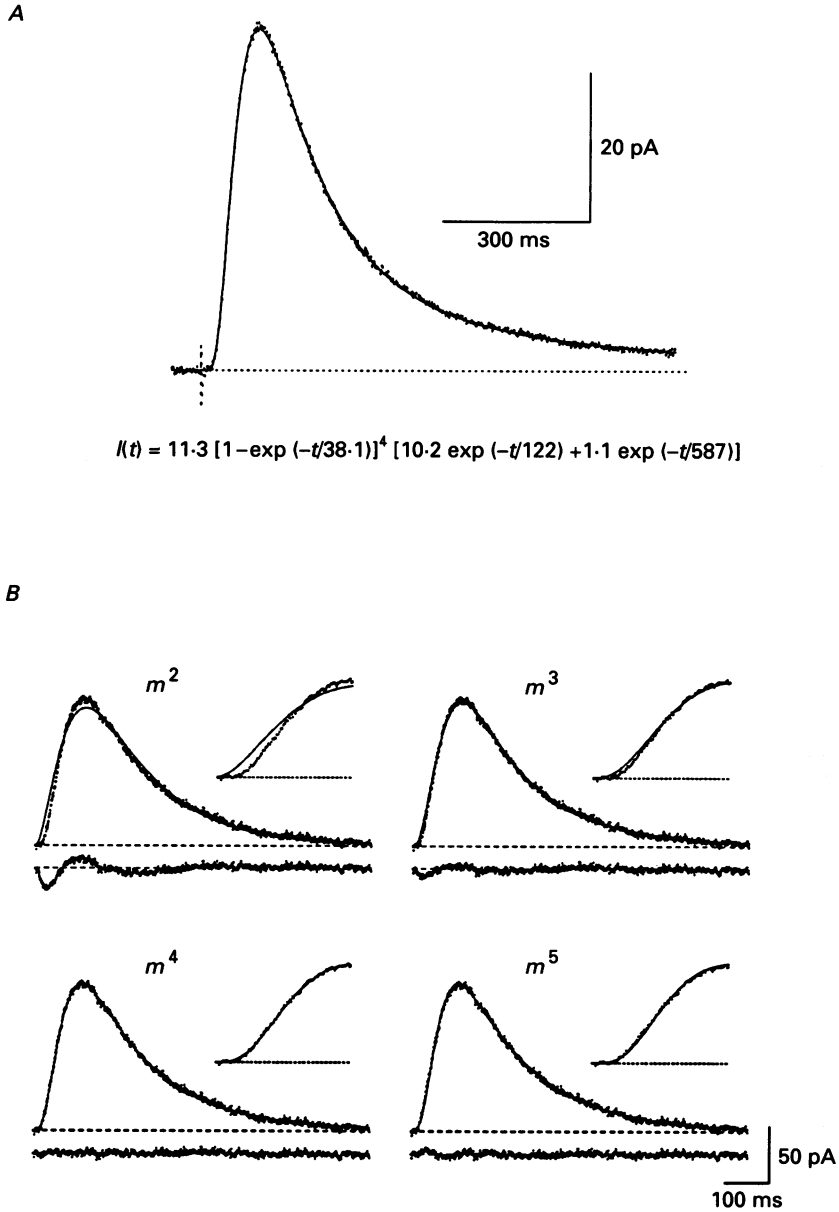

Fig. 2. The postsynaptic $GABA_B$ current is best fitted by an equation using fourth-power exponential activation and double exponential inactivation kinetics $[m^4(h_1+h_2)]$. *A*, an average of the responses is displayed with a fitted curve. Shown below is the equation describing the fit, with an activation time constant (τ_m) of 38·1 ms, and two inactivation time constants (τ_{h_1} and τ_{h_2}) of 122 and 587 ms. *B*, using the fitting algorithm discussed in Methods, curves were generated after varying the exponential power of the activation process from 2 to 5 (from a different cell than in Fig. 2*A*). The inset shows the fit to the rising phase of the current, and the residuals are plotted in the lower trace of each panel. The residuals are minimized by using an m^4 fit.

Figure 2*B* shows that an optimal fit is obtained with fourth-power exponential activation (m^4). Choosing exponents > 4 fitted the rising slope of the current less accurately, independent of the 'lag' (see inset). Such co-operativity was present in all fits to the rising phases, none of which could be described by an equation with an exponent of less than 3 ($n = 39$). Though a high exponent coupled with a smaller

TABLE 1. The mean activation time constant (τ_m), inactivation time constants (τ_{h_1} and τ_{h_2}), and the weighting factors for the inactivation time constants (w_{h_1} and w_{h_2}, respectively) are given for different experimental conditions

	τ_m	τ_{h_1}	τ_{h_2}	w_{h_1}	w_{h_2}	N
			Effects of temperature			
34–35 °C	45·2 ± 0·9	110·2 ± 6·8	516·2 ± 52·5	0·84 ± 0·03	0·16 ± 0·03	19
22–23 °C	112·1 ± 7·8*	282·8 ± 35·5*	1026 ± 134*	0·84 ± 0·03	0·16 ± 0·04	8
			Effects of a competitive antagonist			
Control	51·1 ± 7·5	111·8 ± 18·0	532·8 ± 45·4	0·92 ± 0·02	0·08 ± 0·02	5
CGP 35348	54·8 ± 7·5	91·5 ± 9·6	539·8 ± 66·0	0·89 ± 0·04	0·16 ± 0·04	5
			Paired-pulse, 200 ms ISI			
P_1	45·7 ± 1·1	112·6 ± 6·6	568·8 ± 79·2	0·84 ± 0·03	0·16 ± 0·03	11
P_2	46·2 ± 2·2	96·2 ± 6·0	532·9 ± 54·3	0·85 ± 0·04	0·16 ± 0·04	11

Each value is displayed as mean ± S.E.M. The conditioning (control) and test current in paired-pulse experiments are denoted as P_1 and P_2, respectively. N equals the number of cells for each average measurement. Asterisks signify values that are significantly different from all other time constants within a column as determined using a post-ANOVA multiple-comparison Tukey's test ($P < 0·05$).

'lag' may account for the time course of the current, for the sake of simplicity, and given the kinetic data on G-protein activation (Vuong *et al.* 1984), we adopted the fourth-power model.

Traces from nineteen neurones fitted with m^4, and a double exponential inactivation gave average values of 45·2 ± 0·9 ms for the activation time constant (τ_m), and 110·2 ± 6·8 ms and 516·2 ± 52·5 ms for the two inactivation time constants (τ_{h_1} and τ_{h_2}) (see Table 1). The first inactivation time constant contributed 84 ± 2·7 % (w_{h_1}) and the second inactivation time constant 16 ± 2·6 % (w_{h_2}) of the decay from peak amplitude ($n = 19$).

Under normal conditions, the estimated cytoplasmic concentration of GTP is of the order of 25 μM (Breitweiser & Szabo, 1988). To rule out the possibility that the higher concentrations of GTP (200 μM) in our pipette solutions might somehow alter the kinetics of G-protein-activated currents, kinetics of $GABA_B$ currents were measured in experiments using pipette solutions without exogenous GTP. In such experiments the average activation time constant was 49·5 ± 1·1 ms, and the average inactivation time constants were 125·6 ± 10·6 and 507·9 ± 101·1 ms ($n = 4$), which were not significantly different from values obtained with intracellular GTP present ($P > 0·1$, ANOVA).

The time course of the synaptic $GABA_B$ current was sensitive to temperature (Table 1). Activation and inactivation kinetics measured from granule cells recorded at room temperature allowed rough estimates of the Q_{10} (temperature coefficient) values for τ_m, τ_{h_1} and τ_{h_2} of 2·31, 2·3 and 1·82 respectively.

Finally, the activation and inactivation kinetics were used to calculate the total charge carried by a typical GABA$_B$ response at a membrane potential of −84 mV, the mean resting potential of granule cells (Staley *et al.* 1992). Given a mean peak conductance of 1·52 nS (in 2·5 mM $[K^+]_o$), and an E_K of −98 mV, approximately

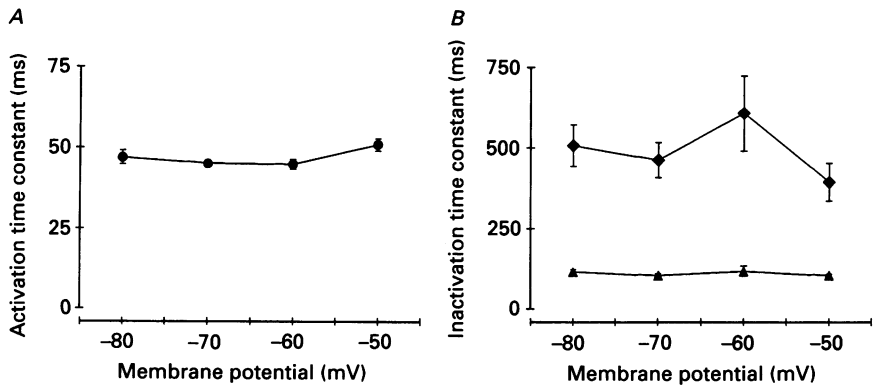

Fig. 3. Neither the time constant of activation (τ_m), nor the inactivation time constants (τ_{h_1} and τ_{h_2}), are voltage dependent between −45 and −85 mV. *A*, activation time constants from fifteen cells have been separated into 10 mV bins and their means are displayed as a function of voltage. *B*, plot of the fast and slow inactivation time constants measured in the same cells. Regression analysis showed no significant voltage dependence to the activation or inactivation time constants.

7·8 pC leave the cell. This compares to a range of 8·8–35·1 pC carried by a typical stimulus-evoked GABA$_A$ current (see Otis & Mody, 1992*b*, and Staley & Mody, 1992), given an E_{Cl} of −70 mV.

The effects of membrane potential on the activation and inactivation kinetics

The activation and inactivation kinetics derived from similar fits were independent of voltage in the range of −45 to −95 mV. Activation time constants and inactivation time constants measured at different holding potentials were sorted into four separate bins. The resulting plots are displayed in Fig. 3*A* and *B*, and regression analyses reveal no significant voltage dependence of τ_m (Fig. 3*A*) or τ_{h_1} and τ_{h_2} (Fig. 3*B*).

Paired-pulse depression of the GABA$_B$ current

In each paired-pulse experiment a conditioning current and a test current elicited by identical stimuli were separated by different interstimulus intervals (ISIs). Because of the slow time to peak and the extremely slow decay of the GABA$_B$ currents, the conditioning and test currents often overlapped in time (see Fig. 4*A*), and for short ISIs, the conditioning current had not reached its peak before the test stimulus was delivered. To obtain accurate values for the peak of the test GABA$_B$ current, a subtraction procedure was employed and is graphically illustrated in Fig. 4*A* and *B*. Digitally subtracting the single-pulse trace from the paired-pulse trace gives the difference trace displayed in Fig. 4*B*, from which the peak amplitude and

kinetic profile of the test current can be accurately measured. In this way, paired-pulse data from fourteen cells with ISIs ranging from 50 to 5000 ms were calculated and are displayed in Fig. 4*C*. In addition, paired-pulse depression measurements from $GABA_A$ responses ($n = 4$–9) are superimposed (also see Otis & Mody, 1992*a*), to

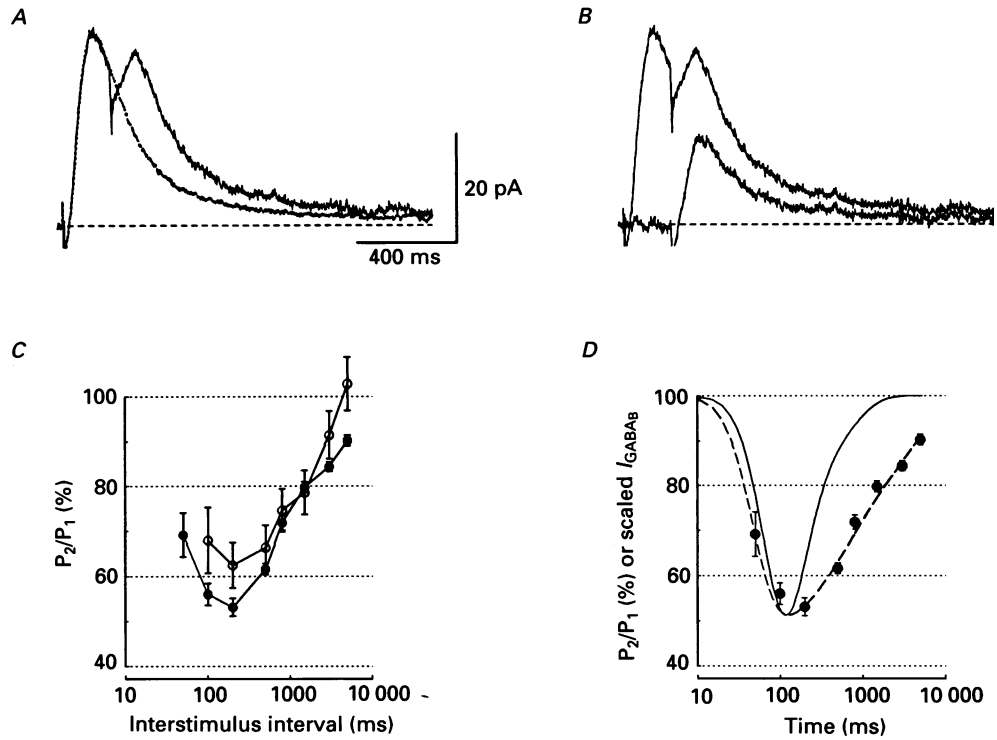

Fig. 4. The time course of the paired-pulse depression is similar for the $GABA_A$ and $GABA_B$ currents, but a presynaptic conductance identical to the postsynaptic $GABA_B$ current cannot account by itself for this depression. *A*, the displayed, paired-pulse trace was elicited by a conditioning and a test stimulus, separated by 200 ms. The other trace is an average response to a single stimulus. *B*, subtracting the response to a single stimulus in *A* from the response to paired stimuli yields the trace representing the true test response, shown here along with the original paired-pulse response. All of the paired-pulse measurements were made after employing this method so that accurate peak amplitudes of the test responses could be obtained, and the true time course of the test response could be observed. Stimulating artifacts have been truncated. *C*, the peak amplitude of test currents (P_1) normalized to the peak amplitude of conditioning currents (P_2) has been plotted *versus* the inter-stimulus interval for both the $GABA_A$ responses (○, $n = 4$–9 cells) and for the $GABA_B$ responses (●, $n = 14$). Mean paired-pulse depression measured for each response showed a very similar time course, with no significant differences between values at each interstimulus interval ($P > 0{\cdot}1$, ANOVA). *D*, a theoretical trace representing the postsynaptic $GABA_B$ current was generated according to the average kinetics values using the equation described in the text. This trace is superimposed on the data obtained from the paired-pulse depression of the $GABA_B$ current. The dashed line is a curve of the same form as that used to describe the postsynaptic current which has been fitted to the data of the paired-pulse depression (see text for details). This dashed line is meant to represent the time course of putative $GABA_B$-mediated presynaptic mechanism(s) responsible for the paired-pulse depression.

highlight their similar time courses. The slight differences apparent at short ISIs (100 and 200 ms) are not significant ($P > 0{\cdot}1$, ANOVA).

Figure 4*D* provides a useful comparison that can rule out the possibility that a GABA$_B$ receptor-activated presynaptic K^+ current identical to the postsynaptic

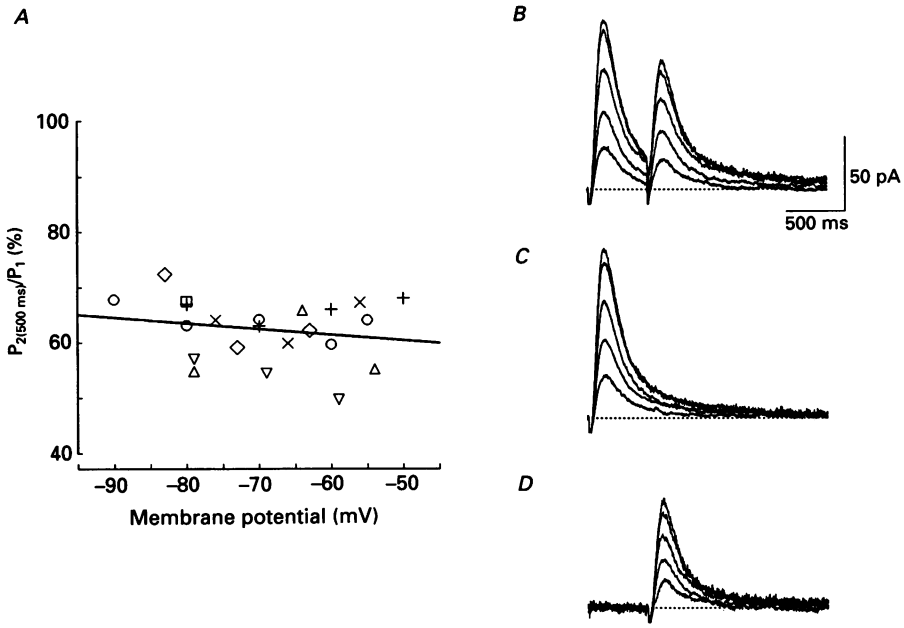

Fig. 5. The paired-pulse depression is independent of postsynaptic membrane voltage. *A*, the percentage paired-pulse depression measured at 500 ms ($P_{2(500\ ms)}/P_1$) as a function of voltage in seven different neurones. Each symbol represents measurements at different voltages within a given cell. The equation for the regression line is $y = 0{\cdot}1\%\ mV^{-1}\ x + 55{\cdot}3\%$, demonstrating that for a 10 mV depolarization the normalized depression would increase by only 1%. The slope is not significantly different from 0 ($P > 0{\cdot}1$, ANOVA). *B*, *C* and *D* display average traces at a different holding potentials (from the top trace: −54, −59, −69, −79 and −89 mV, ○ in *A*) for the paired-pulse, a single-stimulus, and the difference trace (paired-pulse trace minus single-stimulus trace), respectively.

response is sufficient to account for the presynaptic inhibition. A theoretical GABA$_B$ current (generated from the average kinetic data obtained from the fits) has been inverted and normalized (Fig. 4*D*). Also displayed in Fig. 4*D* is a dashed line of the same general mathematical form as that fitted to the GABA$_B$ currents,

$$100\{1-0{\cdot}75[1-\exp(-t/24{\cdot}3)]^4\,[0{\cdot}35\exp(-t/53{\cdot}5)+0{\cdot}40\exp(-t/4191)]\},$$

but which has been fitted to the GABA$_B$ paired-pulse depression values shown in Fig. 4*C*. The two curves peak at approximately the same time (~ 150 ms), but the depression lasts considerably longer than the postsynaptic conductance.

If paired-pulse depression is entirely due to presynaptic inhibition then it should be independent of the postsynaptic membrane potential. Indeed, this was the case between −50 and −90 mV (Fig. 5). The slope of the regression line fitted to the individual measurements taken from seven different cells is not statistically

significant from 0% mV^{-1} ($P > 0{\cdot}1$, ANOVA; Fig. 5*A*). Individual traces from a single experiment are shown in Fig. 5*B*, *C* and *D*, demonstrating representative paired-pulse traces, single-pulse traces, and difference (test-pulse) traces respectively.

Kinetics of the $GABA_B$ current in the presence of a competitive antagonist, and during the paired-pulse depression

The kinetics of the current were invariant as the presumed competitive antagonist CGP 35348 partially blocked the $GABA_B$ receptors. Figure 6*A* (top), shows two

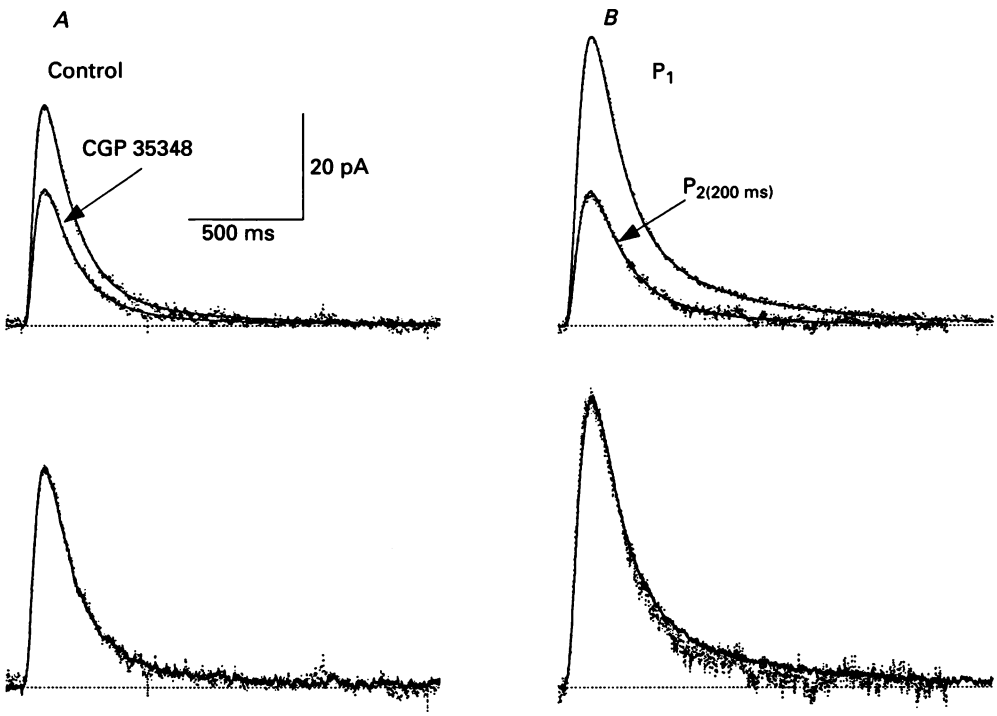

Fig. 6. The kinetics of the $GABA_B$ current are not altered by partial antagonism by CGP 35348, or by a preceding conditioning stimulus. *A*, an average control trace, and an average trace taken during the wash in of 200 μM CGP 35348 are displayed, each superimposed by a fitted curve. Below, the CGP trace has been normalized and plotted as single points over the control response to show that despite 40% antagonism by CGP 35348, the two traces have identical time courses. *B*, the conditioning pulse (P_1) and the test pulse $P_{2(200ms)}$, from a 200 ms paired-pulse experiment performed in a different granule cell. Both traces have fitted curves displayed as well. In the lower panel, the test pulse has been normalized to the conditioning pulse to show that they have identical time courses.

average traces, one taken during a control period (continuous line) and the other during partial blockade of the current by CGP 35348 (dotted line). The normalized traces are superimposed in the bottom part of Fig. 6*A* to show their identical time courses. Curves fitted to average responses during an approximate 50% (mean 50·6%) blockade of the current differed in activation and inactivation kinetics by less than 10% from curves fit to control traces in the same cells ($n = 5$, see Table 1).

These data are consistent with the idea that a competitive antagonist does not affect any steps in the transduction cascade which occurs after transmitter binds to the receptor.

In Fig. 6*B* (top), traces and fitted curves are displayed for a single pulse, together with a trace obtained by subtracting the single-pulse trace from a 200 ms ISI paired-pulse trace. Fits from eleven cells showed that, as is the case for competitive antagonism by CGP 35348, paired-pulse depression occurs without any statistically significant change in the activation or inactivation kinetics of the conductance (Table 1). In the bottom panel of *B*, the test pulse (P_2) has been scaled to the conditioning pulse (P_1), emphasizing the similarity in their time courses (see also Table 1). Thus, it is unlikely that some desensitization process takes place during the paired-pulse depression, as such a process would have to occur without affecting the kinetics of the current.

DISCUSSION

In this study, we have pharmacologically isolated the $GABA_B$-mediated K^+ current in response to synaptically released transmitter and characterized its basic voltage dependence, reversal potential and kinetics. The results obtained here are not confounded by the use of exogenous agonists which may elicit responses which do not solely result from the activation of $GABA_B$ receptors (Jarolimek & Misgeld, 1992). The synaptic currents were most probably a result of $GABA_B$ receptor activation, as they were antagonized by CGP 35348 (Olpe *et al.* 1990), and by intracellular QX-314 (Nathan *et al.* 1990; Otis & Mody, 1992*a*) or Cs^+ ions (Gähwiler & Brown, 1985; Otis & Mody, 1992*a*).

Current–voltage relationship and kinetics of the $GABA_B$ current

In the voltage range between spike threshold of granule cells (−49 mV) (Staley *et al.* 1992) and hyperpolarized (−110 mV) to the E_K, there was little evidence for rectification of the $GABA_B$-activated conductance. Though it has been suggested that the $GABA_B$ current is reduced at depolarized membrane potentials (Gähwiler & Brown, 1985; Crunelli & Leresche, 1991), we found no rectification of the outward $GABA_B$ currents in granule cells from the dentate gyrus. In fact, in contrast to the inward rectification described by Gähwiler & Brown (1985), the rectification observed in our study upon hyperpolarization and in 6·8 mM $[K^+]_o$, was in the outward direction.

Possible explanations for the above discrepancies include the use in previous studies of sharp microelectrode voltage clamp, which may have resulted in the underestimation of holding potentials at depolarized voltages or in the occurrence of some unclamped conductances obscuring the $GABA_B$ current. Another possibility is that $GABA_B$ receptors may be coupled to different types of K^+ channels in different neurones (CA3 pyramidal cells *vs.* granule cells). It should also be noted that synaptic $GABA_B$ responses, as opposed to conductances activated by an exogenous agonist such as baclofen, do not seem to rectify (Thalmann, 1988; Davies *et al.* 1990).

Single-channel studies may provide an answer to the question of rectification. Of three studies examining G-protein-activated K^+ channels (VanDongen *et al.* 1988; Miyake *et al.* 1989; Premkumar *et al.* 1991), two show inwardly rectifying single-

channel conductances (Miyake *et al.* 1989; Premkumar *et al.* 1991) in response to exogenously applied agonists. The third study (VanDongen *et al.* 1988) characterizes a group of 38 pS channels which pass current only in the inward direction, as well as a 13 pS channel and a 55 pS channel which show a linear I–V relationship. These channels were directly activated in hippocampal neurones by the G_o α-subunit. Thus, it is possible that the responses recorded in our study result from either or both of the non-rectifying 13 and 55 pS channels, while exogenous agonists may also activate the other class of rectifying 38 pS channels.

The kinetics of the $GABA_B$ current are unlike those reported for any fast synaptic current. The 'lag' may result from a G-protein cascade occurring prior to channel activation, and the fourth-power exponential relationship may reflect the level of co-operativity in the transduction mechanism. There is precedent for fourth-power co-operativity in K^+ channel activation (Hille, 1968), which could result from the interaction of the four subunits thought to be necessary for the constitution of a functional K^+ channel (Mackinnon, 1991). The simplest model of $GABA_B$ receptor-associated K^+ channel gating would contain four distinct closed states, one open state, and two processes of inactivation. Co-operative activation may stem from multiple closed states of the channel or may reflect the requirement for the binding of four G-protein subunits to the channel.

Two pathways for channel closure could account for the inactivation processes. Of the two, the slow rate of inactivation is comparable to the rate of GTP hydrolysis estimated for the muscarinic receptor-activated cardiac inwardly rectifying K^+ channel ($I_{K(M)}$; Breitwieser & Szabo, 1988). Thus, the decline of GTP-bound G-protein levels may account for the slow, second component of $GABA_B$ current inactivation. Finally, the temperature dependence of synaptic $GABA_B$ response kinetics are in good agreement with previously estimated Q_{10} values (2·2–2·3) obtained from experiments on a presumed G-protein-activated, non-rectifying K^+ conductance in invertebrate neurones (Brezina, 1988).

Our measurements of peak $GABA_B$ conductance varied between 0·8 and 6·4 nS, a small conductance compared with the 5–20 nS peak $GABA_A$ conductance recorded in these cells (Otis & Mody, 1992*b*), but consistent with its suggested function to reactivate voltage-inactivated conductances (Crunelli & Leresche, 1991), or to provide hyperpolarizing inhibition (Misgeld *et al.* 1989). However, when the total charge carried by the $GABA_B$ current is considered, the long duration of the current allows small amplitude responses to move a substantial amount of charge, comparable to the amount of charge carried by chloride ions during small evoked $GABA_A$ responses.

Paired-pulse depression

Paired-pulse depression has been described for both synaptic GABA responses, and is thought to result from presynaptic inhibition, mediated through $GABA_B$ receptors (Davies *et al.* 1990). However, both depressions need not be due to the same mechanisms because different populations of inhibitory neurones may be responsible for $GABA_A$ and $GABA_B$ responses (Segal, 1990; Otis & Mody, 1992*a*). In the absence of pharmacological tools (Davies *et al.* 1990; Otis & Mody, 1992*a*), the hypothesis that depression of the $IPSP/C_B$ response is due to presynaptic inhibition relies solely

on the observation that the time course of the depression is similar for both $GABA_A$ and $GABA_B$ components (Davies *et al.* 1990; and present study).

Our findings that the kinetics of $GABA_B$ responses are unaltered by a conditioning stimulus, and that there is no voltage dependence to the paired-pulse depression strengthens the argument that this process is due to a reduction in transmitter release. Any postsynaptic mechanism for paired-pulse depression would require some inhibition at a point in the transduction pathway prior to channel activation. Though unlikely, this is still plausible, and could result from a modification of the receptor, as is the case for the G-protein-coupled receptor rhodopsin which, a short time after it is activated is phosphorylated in order to stop its activity (Wilden, Hall & Kuhn, 1986). Alternatively, the G-protein might be inhibited in some way without affecting the rate of activation of the macroscopic current.

Finally, it is of obvious interest what constitutes the ionic or second messenger mechanism of the presynaptic inhibition. The two leading hypotheses are a direct inhibition of presynaptic calcium current, or a hyperpolarization of the presynaptic cell/terminal (Misgeld *et al.* 1989; Harrison *et al.* 1988; but see Gage, 1992), leading to reduced transmitter release. Our data indicate that the hyperpolarization cannot be mediated exclusively by a presynaptic $GABA_B$ conductance with the kinetics described in this study. While the postsynaptic $GABA_B$ K^+ current rises with a similar time course, it decays too quickly to give rise to a long presynaptic hyperpolarization. Though a very short presynaptic membrane time constant could preserve the fast time to the peak of the paired-pulse depression (150 ms), a very long time constant (> 5 s) would be necessary to provide a sufficiently long hyperpolarization. It is nevertheless possible that a barium-sensitive K^+ current (Thompson & Gähwiler, 1992), with substantially different kinetics, might underlie a critical presynaptic hyperpolarization. Likewise, paired-pulse depression may be explained by a presynaptic hyperpolarization coupled with a longer lasting secondary process (Gage, 1992), such as an inhibition of transmitter release subsequent to calcium influx, or the slow inactivation of presynaptic terminal intrinsic currents, and an increase in the presynaptic membrane time constant. Alternatively, direct inhibition of a calcium current could by itself account for the entire paired-pulse depression (Dunlap & Fischbach, 1981; Scholz & Miller, 1991). The resolution of these issues will require recordings from GABAergic interneurones or their terminals.

We would like to thank Drs David Prince and John Huguenard for helpful comments on the manuscript, as well as Dr Denis Baylor for helpful discussions. Jim Palmer provided indispensable technical assistance. T.S.O. is supported by a Howard Hughes Predoctoral Fellowship. Y.D.K. is a fellow of the Canadian MRC. This work was supported by NINDS grants NS-12151, N-27528 and a Klingenstein Foundation Fellowship to I.M.

REFERENCES

BOWERY, N. G., HILL, D. R., HUDSON, A. L., DOBLE, A., MIDDLEMISS, D. N., SHAW, J. & TURNBULL, M. (1980). (−)-Baclofen decreases neurotransmitter release in mammalian CNS by an action at a novel GABA receptor. *Nature* **283**, 92–94.

BOWERY, N. (1989). $GABA_B$ receptors and their significance in mammalian pharmacology. *Trends in Pharmacological Sciences* **10**, 401–407.

BREITWIESER, G. E. & SZABO, G. (1988). Mechanism of muscarinic receptor-induced K^+ channel activation as revealed by hydrolysis-resistant GTP analogues. *Journal of General Physiology* **91**, 469–493.

BREZINA, V. (1988). Guanosine 5′-triphosphate analogue activates potassium current modulated by neurotransmitters in *Aplysia* neurones. *Journal of Physiology* **407**, 15–40.

CACECI, M. S. & CACHERIS, W. P. (1984). Fitting curves to data: the simplex algorithm is the answer. *Byte* **9**, 340–362.

CRUNELLI, V. & LERESCHE, N. (1991). A role for $GABA_B$ receptors in excitation and inhibition of thalamocortical cells. *Trends in Neurosciences* **14**, 16–21.

DAVIES, C. H., DAVIES, S. N. & COLLINGRIDGE, G. L. (1990). Paired-pulse depression of monosynaptic GABA-mediated inhibitory postsynaptic responses in rat hippocampus. *Journal of Physiology* **424**, 513–531.

DEISZ, R. A. & PRINCE, D. A. (1989). Frequency-dependent depression of inhibition in guinea-pig neocortex *in vitro* by $GABA_B$ receptor feed-back on GABA release. *Journal of Physiology* **412**, 513–542.

DUNLAP, K. & FISCHBACH, G. D. (1981). Neurotransmitters decrease the calcium conductance activated by depolarization of embryonic sensory neurones. *Journal of Physiology* **317**, 519–535.

DUTAR, P. & NICOLL, R. A. (1988*a*). A physiological role for $GABA_B$ receptors in the central nervous system. *Nature* **332**, 156–158.

DUTAR, P. & NICOLL, R. A. (1988*b*). Pre- and postsynaptic $GABA_B$ receptors in the hippocampus have different pharmacological properties. *Neuron* **12**, 585–591.

GÄHWILER, B. H. & BROWN, D. A. (1985). $GABA_B$ receptor-activated K^+ current in voltage-clamped CA3 pyramidal cells in hippocampal cultures. *Proceedings of the National Academy of Sciences of the USA* **82**, 1558–1562.

GAGE, P. W. (1992). Activation and modulation of neuronal potassium channels by GABA. *Trends in Neurosciences* **15**, 46–51.

GILMAN, A. G. (1987). G-proteins: Transducers of receptor-generated signals. *Annual Review of Biochemistry* **56**, 615–649.

HARRISON, N. L. (1990). On the presynaptic action of baclofen at inhibitory synapses between cultured rat hippocampal neurones. *Journal of Physiology* **422**, 433–446.

HARRISON, N. L., LANGE, G. D. & BARKER, J. L. (1988). (−)Baclofen activates presynaptic $GABA_B$ receptors on GABAergic inhibitory neurons from embryonic rat hippocampus. *Neuroscience Letters* **85**, 105–109.

HILLE, B. (1968). Charges and potentials at the nerve surface: Divalent ions and pH. *Journal of General Physiology* **51**, 221–236.

JAROLIMEK, W. & MISGELD, U. (1992). On the inhibitory actions of baclofen and γ-aminobutyric acid in rat ventral midbrain culture. *Journal of Physiology* **451**, 419–443.

LACAILLE, J.-C. (1991). Postsynaptic potentials mediated by excitatory and inhibitory amino acids in interneurones of stratum pyramidale of the CA1 region of rat hippocampal slices in vitro. *Journal of Neurophysiology* **66**, 1441–1454.

MACKINNON, R. (1991). Determination of subunit stoichiometry of a voltage activated potassium channel. *Nature* **350**, 232–235.

MISGELD, U., MÜLLER, W. & BRUNNER, H. (1989). Effects of (−)baclofen on inhibitory neurons in the guinea pig hippocampal slice. *Pflügers Archiv* **414**, 139–144.

MIYAKE, M., CHRISTIE, M. J. & NORTH, R. A. (1989). Single potassium channels opened by opioids in rat locus ceruleus neurons. *Proceedings of the National Academy of Sciences of the USA* **86**, 3419–3422.

NATHAN, T., JENSEN, M. S. & LAMBERT, J. D. C. (1990). The slow inhibitory postsynaptic potential in rat hippocampal neurons is blocked by intracellular injection of QX-314. *Neuroscience Letters* **110**, 309–313.

NEWBERRY, N. R. & NICOLL, R. A. (1985). Comparison of the actions of baclofen with GABA on rat hippocampal pyramidal cells *in vitro*. *Journal of Physiology* **360**, 161–185.

NICOLL, R. A., MALENKA, R. C. & KAUER, J. A. (1990). Functional comparison of neurotransmitter receptor subtypes in mammalian central nervous system. *Physiological Reviews* **70**, 513–565.

OLPE, H. R., KARLSSON, G., POZZA, M. F., BRUGGER, F., STEINMANN, M., VAN RIEZEN, H., FAGG, G., HALL, R. G., FROESTL, W. & BITTIGER, H. (1990). CGP 35348: a centrally active blocker of $GABA_B$ receptors. *European Journal of Pharmacology* **187**, 27–38.

OTIS, T. S. & MODY, I. (1992*a*). Differential activation of $GABA_A$ and $GABA_B$ receptors by spontaneously released transmitter. *Journal of Neurophysiology* **67**, 222–230.

OTIS, T. S. & MODY, I. (1992*b*). Modulation of the decay kinetics and frequency of spontaneous $GABA_A$ postsynaptic currents. *Neuroscience* **49**, 13–32.

OTIS, T. S., STALEY, K. J. & MODY, I. (1991). Perpetual inhibitory activity in mammalian brain slices generated by spontaneous GABA release. *Brain Research* **545**, 142–150.

PREMKUMAR, L. S., CHUNG, S.-H. & GAGE, P. W. (1990). GABA-induced potassium channels in cultured neurons. *Proceedings of the Royal Society* B**241**, 153–158.

SCHOLZ, K. P. & MILLER, R. J. (1991). $GABA_B$ receptor-mediated inhibition of Ca^{2+} currents and synaptic transmission in cultured rat hippocampal neurons. *Journal of Physiology* **444**, 669–686.

SEGAL, M. (1990). A subset of local interneurones generated slow inhibitory postsynaptic potentials in hippocampal neurons. *Brain Research* **511**, 163–164.

STALEY, K. J. & MODY, I. (1992). Shunting of excitatory input to dentate gyrus granule cells by a depolarizing $GABA_A$ receptor-mediated postsynaptic conductance. *Journal of Neurophysiology* **68**, 197–212.

STALEY, K. J., OTIS, T. S. & MODY, I. (1992). Membrane properties of dentate gyrus granule cells: comparison of sharp microelectrode and whole cell recordings. *Journal of Neurophysiology* **678**, 1346–1358.

THALMANN, R. H. (1988). Evidence that guanosine triphosphate (GTP)-binding proteins control a synaptic response in brain: effects of pertussis toxin and GTPγS on the late inhibitory postsynaptic potential of hippocampal CA3 neurons. *Journal of Neuroscience* **8**, 4589–4602.

THOMPSON, S. M. & GÄHWILER, B. H. (1992). Comparison of the actions of baclofen at pre- and postsynaptic receptors in the rat hippocampus *in vitro*. *Journal of Physiology* **451**, 329–345.

VANDONGEN, A. M. J., CODINA, J., OLATE, J., MATTERA, R., JOHO, R., BIRNBAUMER, L. & BROWN, A. M. (1988). Newly identified brain potassium channels gated by the guanosine nucleotide binding protein G_o. *Science* **242**, 1433–1437.

VANYSEK, P. (1988). Activity coefficients for acids, bases and salts. In *Handbook of Chemistry and Physics*, ed. WEAST, R. C., p. D-169. CRC Press, Boca Raton, FL, USA.

VUONG, T. M., CHABRE, M. & STRYER, L. (1984). Millisecond activation of transducin in the cyclic nucleotide cascade of vision. *Nature* **311**, 659–661.

WILDEN, U., HALL, S. W. & KUHN, H. (1986). Phosphodiesterase activation by photoexcited rhodopsin is quenched when rhodopsin is phosphorylated and binds 48 Kd-protein. *Proceedings of the National Academy of Sciences of the USA* **83**, 1174–1178.

YATANI, A., MATTERA, R., CODINA, J., GRAF, R., OKABE, K., PADRELL, E., IYENGAR, E., BROWN, A. & BIRNBAUMER, L. (1988). The G-protein gated atrial K^+ channel is stimulated by three distinct G_i α-subunits. *Nature* **336**, 680–682.